

Sensor and Simulation Notes

Note 342

June 1992

A Canonical Scatterer for Transient Scattering Range Calibration

Everett G. Farr
Farr Research
Albuquerque, NM 87123

Carl E. Baum
Phillips Laboratory
Albuquerque, NM 87117

CLEARED
FOR PUBLIC RELEASE
PL/PA 6-12-92

Abstract

We describe here a simple process for calibrating a transient scattering range. The process uses a paraboloidal scatterer to transform an axially incident plane wave into a spherical wave. Since the magnitude of the scattered field is known analytically, one can simply calibrate a measurement system. In order to calculate the scattered field, we use a stereographic projection that has previously been called the reflector transform.

This technique provides three advantages over traditional calibration with a sphere. First, it is potentially more accurate, since the scattering characteristics of a paraboloid are independent of frequency. There is no need to convert the measured time domain data to the frequency domain in order to deconvolve the characteristics of the scatterer; the entire process takes place in the time domain. Second, this technique is simpler to implement. Finally, this technique is appropriate for certain anechoic chambers built of two-wire and four-wire transmission lines, where the incident field is not quite uniform.

PL 92-0422

I. Introduction

When measuring the transient scattering properties of an object, it is useful to compare the measured results to a known standard; a scatterer with well-known and simply calculable properties. Current practice is to use a sphere as a known object for surface field measurements and for scattering, and deconvolve the frequency dependence of the sphere from the measurement [1,2]. We propose here an alternative scatterer particularly well suited to time domain measurements, a parabola of revolution, or paraboloid. This method should be simpler to implement than earlier methods, and may also be more accurate. In addition, it handles certain new anechoic chamber designs, in which the incident field is slightly nonuniform.

The idea behind this paper is very simple. If a plane wave is incident upon a convex paraboloid from the end-on direction, then a spherical wave is reflected from the paraboloid. The magnitude of the scattered spherical wave is proportional to $2F/(r(1+\cos(\theta)))$, where F is the focal length of the parabola, θ is the spherical angle from the z axis, and the incident plane wave approaches from an angle of $\theta=0$. This result is true until the edges of the paraboloid become apparent in the measurement. A diagram showing an approximate experimental layout is shown in Figure 1. The frequency dependence is flat and accurate over a theoretically infinite frequency range.

The importance of this new calibration process is its potential for higher accuracy. Normally, one would have to make measurements in the time domain, convert these to the frequency domain, remove the frequency-dependent properties of the scatterer (e.g., a sphere), and inverse transform back into the time domain. With the new calibration technique, the calibration process remains entirely in the time domain, since the scattering properties of the paraboloid are independent of frequency. As an added bonus, not only is the frequency response flat, but it is also trivial to calculate.

We point out that a parabola of revolution, or paraboloid, is the same shape as is used in many reflector antennas. The difference is that the new technique uses the convex side of the paraboloid, rather than the concave side. Thus, the shape we propose here is not particularly exotic, nor should it be difficult to build.

Since we envision this method as a replacement for calibration with a sphere, perhaps it is worthwhile to comment on why a sphere is currently used in time domain range calibrations. It seems likely that the use of a sphere carried over from frequency domain measurements. In the frequency domain, the sphere is the only finite-size target one can use whose properties are simply calculable. In the time domain, however, it is unnecessary to have a finite target. One can very easily use some portion of an infinite target, and time-gate away the edges of the target. In the frequency domain, it is possible to time-gate away the edge of a finite paraboloid, but this can be done only with extensive signal processing. Thus, the new technique is less attractive in the frequency domain.

A large part of this paper deals with the calculation of the scattered spherical wave from the paraboloid. A very similar problem was solved in [3]. However, in that paper a spherical

wave was incident from the concave side of a paraboloid, generating a plane wave scattered field. To generate the proof in [3], a stereographic transformation was invoked, which was dubbed the reflector transform. In this paper we use a similar approach

Finally, we note that problems very similar to the current one have been solved in [4,5]. In these works, the solution is confined to uniform plane-wave incidence. Although that is all that is needed for a simple scattering range calibration, the solution we present here is general for arbitrary (nonuniform) plane-wave incidence. This makes the calibration of certain other geometries feasible. These new geometries include new methods of building anechoic chambers using two-wire and four-wire transmission-line structures.

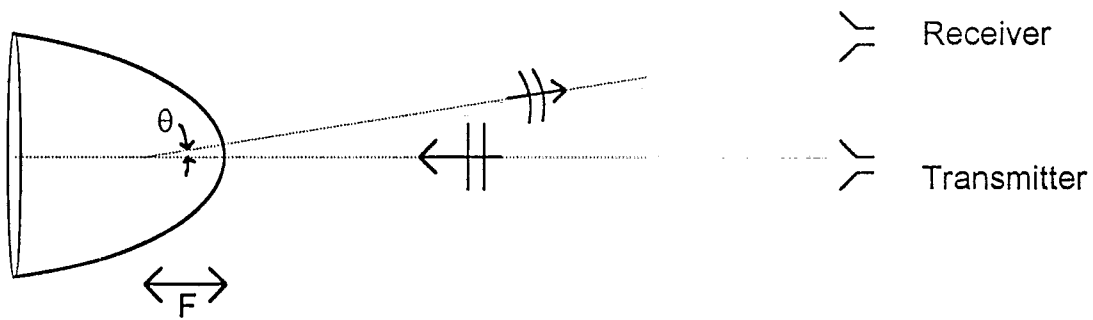


Figure 1. Basic setup for transient scattering range calibration.

II. Scattering of a Uniform Plane Wave with Axial Incidence on a Convex Paraboloid

Let us consider a transient uniform plane wave axially incident upon a paraboloid of focal length F , as shown in Figure 2. The paraboloid may be expressed as

$$r_p = \frac{2F}{1 + \cos(\theta_p)} \quad (2.1)$$

where the coordinate system is centered on the focus of the parabola. Note that the geometry is rotationally symmetric about the z axis. The subscript p indicates a location on the paraboloid. Alternatively, the paraboloid may be expressed as

$$z_p = F - \frac{\Psi_p^2}{4F} \quad (2.2)$$

where Ψ is the radial cylindrical coordinate. A third representation of the paraboloid is

$$\Psi_p = 2F \tan(\theta_p / 2) \quad (2.3)$$

This expression is identical to the stereographic transform of [3, 6-9]. This fact allows the simple form for the scattered field. We will use all three of these representations of the paraboloid in the derivations to follow. Finally, we note a relationship that will come in handy later

$$r_p + z_p = 2F \quad (2.4)$$

This will allow us to simplify the expression for the scattered field.

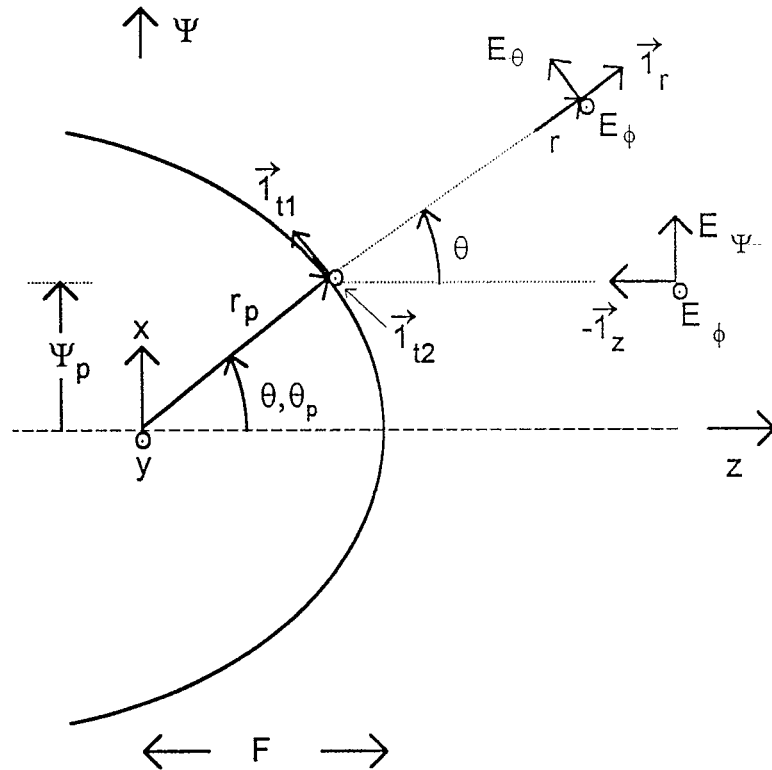


Figure 2. The geometry to be analyzed.

Let us now define the incident field as

$$\vec{E}^{(inc)}(\Psi, \phi, z, t) = -\nabla_{\Psi, \phi} V(\Psi, \phi) f(t+z/c) \quad (2.5)$$

where the transverse gradient function in cylindrical coordinates is

$$\nabla_{\Psi, \phi} = \bar{1}_{\Psi} \frac{\partial}{\partial \Psi} + \bar{1}_{\phi} \frac{1}{\Psi} \frac{\partial}{\partial \phi} \quad (2.6)$$

This describes an arbitrary (not necessarily uniform) plane wave incident along the -z direction. In the next section, we specialize the above expression to uniform plane wave incidence, which is the primary case of interest for the scattering range. Combining the above two equations, we find the incident field as

$$\vec{E}^{(inc)}(\Psi, \phi, z, t) = \left[-\bar{1}_{\Psi} \frac{\partial V(\Psi, \phi)}{\partial \Psi} - \bar{1}_{\phi} \frac{1}{\Psi} \frac{\partial V(\Psi, \phi)}{\partial \phi} \right] f(t+z/c) \quad (2.7)$$

We hypothesize now the solution for the scattered field. This solution is an outgoing wave from $\vec{r} = \vec{0}$ which satisfies causality in the time domain, or the radiation condition in the frequency domain. Thus,

$$\vec{E}^{(sc)}(r, \theta, \phi, t) = \frac{1}{r} \nabla_{\theta, \phi} V(\Psi = 2F \tan(\theta/2), \phi) f(t - (r - 2F)/c) \quad (2.8)$$

where the transverse gradient on a unit sphere is

$$\nabla_{\theta, \phi} = \bar{1}_{\theta} \frac{\partial}{\partial \theta} + \bar{1}_{\phi} \frac{1}{\sin(\theta)} \frac{\partial}{\partial \phi} \quad (2.9)$$

and we have made use of the relation $r_p + z_p = 2F$. Thus, a general expression for the scattered field is

$$\vec{E}^{(sc)}(r, \theta, \phi, t) = \left[\bar{1}_{\theta} \frac{1}{r} \frac{\partial V(2F \tan(\theta/2), \phi)}{\partial \theta} + \bar{1}_{\phi} \frac{1}{r \sin(\theta)} \frac{\partial V(2F \tan(\theta/2), \phi)}{\partial \phi} \right] f(t - (r - 2F)/c) \quad (2.10)$$

We now need only demonstrate that the incident electric field tangent to the paraboloid is equal and opposite to the scattered field tangent to the paraboloid. If this is true, then the above solution is the only correct solution, by the uniqueness theorem.

It is necessary to prove that the tangential fields are equal and opposite in two principal orthogonal directions. It is simplest to choose the first of these as being in the ϕ direction, since both the cylindrical and spherical coordinate systems share this direction. Thus, we identify the first principal tangent vector as

$$\bar{\mathbf{t}}_{t1} = \bar{\mathbf{t}}_\phi \quad (2.11)$$

The second principal direction is perpendicular to this, and still tangent to the paraboloid. This turns out to be tangent to a simple parabola in a plane $\phi=\text{constant}$. Thus, the second principal direction is

$$\begin{aligned} \bar{\mathbf{t}}_{t2} &= \bar{\mathbf{t}}_\Psi \cos(\theta_p/2) - \bar{\mathbf{t}}_z \sin(\theta_p/2) \\ &= \bar{\mathbf{t}}_r \sin(\theta_p/2) + \bar{\mathbf{t}}_\theta \cos(\theta_p/2) \end{aligned} \quad (2.12)$$

where θ_p is a θ on the paraboloid.

Let us consider now matching the incident and scattered fields. Since the tangential components of the fields must be equal and opposite on the paraboloid, we have

$$\begin{aligned} \bar{\mathbf{E}}^{(sc)}(r_p, \theta_p, \phi_p, t) \cdot \bar{\mathbf{t}}_{t1} &= -\bar{\mathbf{E}}^{(inc)}(\Psi_p, \phi_p, z_p, t) \cdot \bar{\mathbf{t}}_{t1} \\ \bar{\mathbf{E}}^{(sc)}(r_p, \theta_p, \phi_p, t) \cdot \bar{\mathbf{t}}_{t2} &= -\bar{\mathbf{E}}^{(inc)}(\Psi_p, \phi_p, z_p, t) \cdot \bar{\mathbf{t}}_{t2} \end{aligned} \quad (2.13)$$

Carrying out the dot products for the first principal direction, we find

$$\left. \frac{f(t - (r_p - 2F)/c)}{r_p \sin(\theta_p)} \frac{\partial V(2F \tan(\theta/2), \phi)}{\partial \phi} \right|_{\theta=\theta_p, \phi=\phi_p} = \left. \frac{f(t + z_p/c)}{\Psi_p} \frac{\partial V(\Psi, \phi)}{\partial \phi} \right|_{\Psi=\Psi_p, \phi=\phi_p} \quad (2.14)$$

This is true since $\Psi_p = r_p \sin(\theta_p)$ and $2F - r_p = z_p$. Matching fields along the second principal tangential vector, we find

$$\begin{aligned} \left. \frac{f(t - (r_p - 2F)/c) \cos(\theta_p/2)}{r_p} \frac{\partial V(2F \tan(\theta/2), \phi)}{\partial \theta} \right|_{\theta=\theta_p, \phi=\phi_p} &= \\ \left. f(t + z_p/c) \cos(\theta_p/2) \frac{\partial V(\Psi, \phi)}{\partial \Psi} \right|_{\Psi=\Psi_p, \phi=\phi_p} & \end{aligned} \quad (2.15)$$

In order to simplify this, we note that

$$\Psi_p = 2F \tan(\theta_p/2) \quad (2.16)$$

on the parabola, so

$$\frac{d\Psi_p}{d\theta_p} = \frac{F}{\cos^2(\theta_p/2)} = \frac{2F}{1+\cos(\theta_p)} = r_p \quad (2.17)$$

Thus,

$$\frac{\partial V}{\partial \theta_p} = \frac{\partial V}{\partial \Psi_p} \frac{\partial \Psi_p}{\partial \theta_p} = \frac{\partial V}{\partial \Psi_p} r_p \quad (2.18)$$

and equation (2.15) is satisfied. Therefore, the scattered field we hypothesized in (2.8) is not only the correct solution, but the unique solution.

III. Uniform Plane Wave Incidence

We consider now the practical application of the above theory to uniform plane wave incidence. If a uniform plane wave is incident from $\theta=0$, we may express this as

$$\begin{aligned}\bar{E}^{(inc)}(\Psi, \phi, z, t) &= \bar{1}_y E_o f(t+z/c) \\ &= -\nabla_t V f(t+z/c)\end{aligned}\tag{3.1}$$

where

$$V(x, y) = -E_o y\tag{3.2}$$

or equivalently

$$V(\Psi, \theta) = -E_o \Psi \sin(\phi)\tag{3.3}$$

Next, we substitute $\Psi = 2F \tan(\theta/2)$, as required by (2.7) to find

$$V(\theta, \phi) = -E_o 2F \tan(\theta/2) \sin(\phi)\tag{3.4}$$

Finally, we substitute the above into (2.8), taking the transverse gradient to find

$$\begin{aligned}\bar{E}^{(sc)}(r, \theta, \phi, t) &= \frac{1}{r} \nabla_{\theta, \phi} [-E_o \tan(\theta/2) \sin(\phi)] f(t - (r - 2F)/c) \\ &= -\frac{E_o}{r} \frac{2F}{1 + \cos(\theta)} [\bar{1}_\theta \sin(\phi) + \bar{1}_\phi \cos(\phi)] f(t - (r - 2F)/c)\end{aligned}\tag{3.5}$$

The above is an expression of the scattered field. It is simple, analytic, and exact. The scattered field is proportional to $2F / (r(1 + \cos(\theta)))$.

The calibration approach is now clear. One sends a uniform plane wave incident upon the axis of a paraboloid, and then makes a measurement at some angle θ to the direction of incidence. What one measures is given in (3.5). Since F , ϕ , and θ can be measured with a meter stick, E_o can be found simply, from say the peak magnitude of the measured response. Only two caveats need to be satisfied. First, the paraboloid must be large enough to allow the receiving antenna to see some prominent characteristic of the waveform before effects due to the truncation of the paraboloid become visible. Second, the transmitter should be far enough away from the scatterer that a good approximation of a plane wave is incident upon the paraboloid.

IV. Extension to Nonuniform Plane Waves

There is one additional special case worth considering. This case involves a guided wave such as the two-wire or four-wire waveguide used either by itself [10], or in one of the newer models of anechoic chamber[11-13]. A diagram of the four-wire configuration is shown in Figure 3.

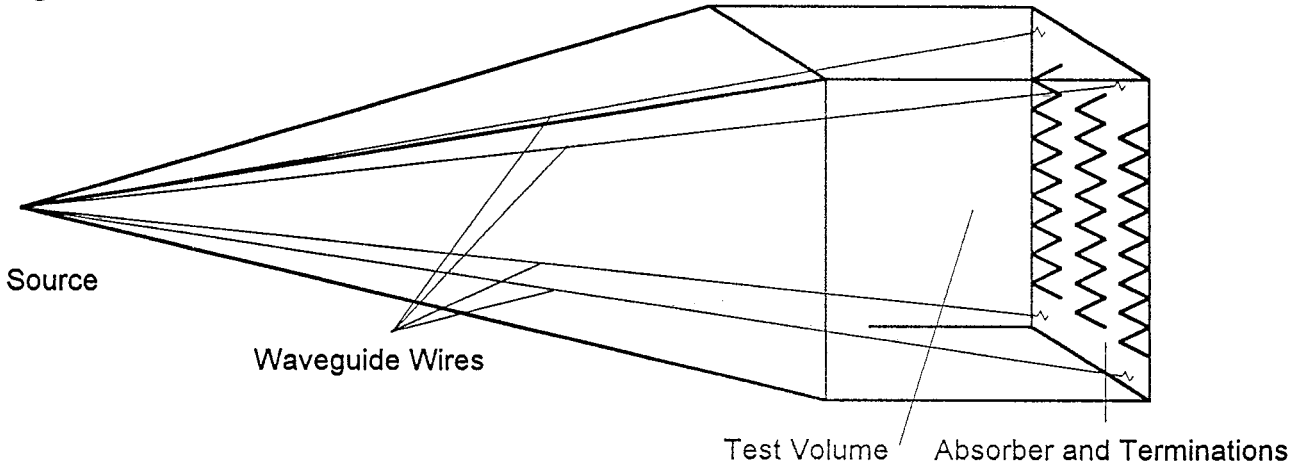


Figure 3. Four-wire anechoic chamber.

In order to calibrate the above range, we note that the phase front in the test volume is approximately planar, assuming a very long feed. Thus, to a good approximation, the incident field in the test volume is the field in a four-wire transmission line, as analyzed in [14] and as shown in Figure 4. The incident plane wave is not quite uniform in the test volume, although it is approximately so. Note that there is a special dimension ratio, $\sqrt{3}$, which provides maximum field uniformity [14]. Alternatively, these chambers are sometimes designed so that the dimension ratio is unity, in order to switch easily between horizontal and vertical polarizations.

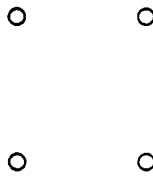


Figure 4. Four wire transmission line.

If one wanted to calibrate the above configuration, the technique developed here would be appropriate. One would only need to express the static potential of the transmission line as a function of position. This function has already been derived in [14], so the process is straightforward. Note that one would normally expect the field in the test volume to be approximately uniform anyway, since that is usually one of the design criteria of a chamber. This suggests that using the exact four wire potential function should introduce only a minor correction into the calibration procedure. A second source of error, which is not dealt with here, is that the incident wave is slightly spherical, rather than planar. We hope to address this issue in a future paper.

V. Truncations Effects

Although the above theory is developed for an infinite paraboloid, in practice a truncated paraboloid will be used. It is worthwhile to identify the clear times involved, in order to specify rigorously how late in time the solution is valid.

Consider the rays shown in Figure 3. If the incident field has a time history of the form $f(t)$, and $f(t) = 0$ for $t < 0$, then the solution is valid out to a time

$$t_{max} = t_3 + t_4 - (t_1 + t_2) \quad (4.1)$$

It is straightforward to calculate each of the times using the definitions of the paraboloid given in equations (2.1)-(2.3).

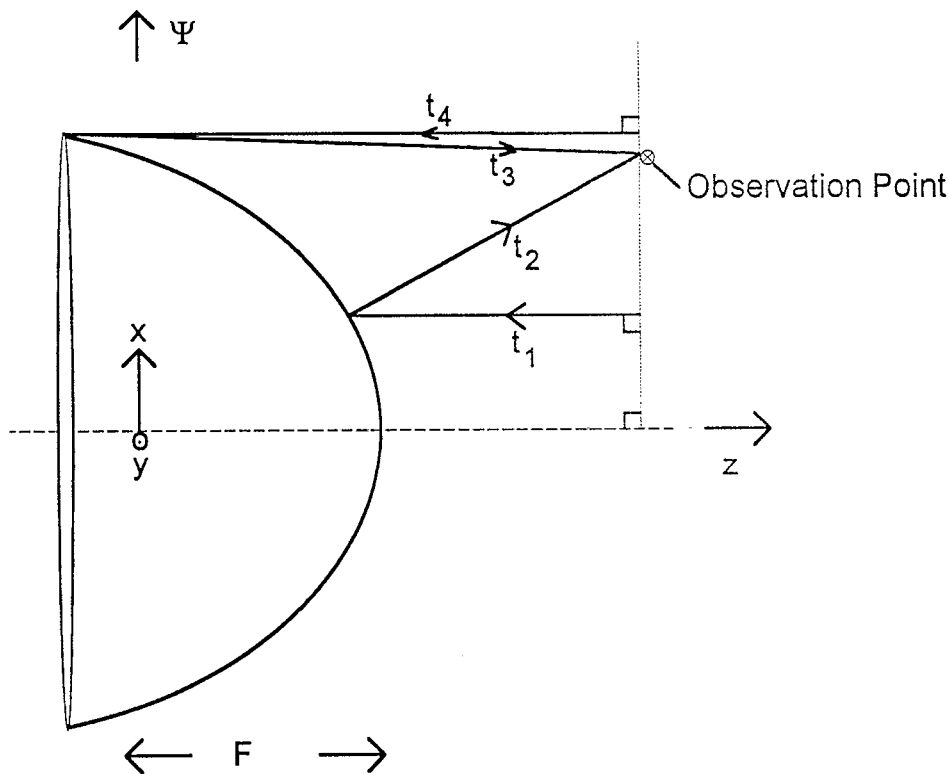


Figure 3. Geometry for calculating clear times.

The conclusion we draw from this is as follows. Some identifiable feature of the radiated waveform (such as the peak) must occur before a time t_{max} has passed since the beginning of the waveform, in order for the calibration technique to work.

VI. Conclusions and Recommendations

A simple method has been described for calibrating a transient scattering range. The method uses a parabola of revolution, or paraboloid, because the scattered field can be expressed in a simple, analytic, exact form.

The new technique provides three advantages over the more traditional method of calibration with a sphere. First, it has the potential for higher accuracy, since the entire calibration process takes place in the time domain. Second, it is simpler to implement, since the scattered field is trivial to calculate. Finally, the technique can handle nonuniform plane waves, such as those occurring in two-wire and four-wire anechoic chambers.

One possible area of future work might involve refining the shape of the paraboloid. The method we have described here is exact and rigorous for plane-wave incidence. In practice, the source is a spherical wave with a large radius of curvature. This is not a very severe restriction, since if one uses a sphere, the same restriction would apply. Nevertheless, it may be possible to refine slightly the shape of the paraboloid to account for this effect, in order to make the calibration technique even more accurate.

References

1. K. S. H. Lee, ed., *EMP Interaction: Principles, Techniques, and Reference Data*, Hemisphere, 1986, Section 1.5.2.
2. R. G. Madonna, "Calibration and Measurement Issues for RCS Measurements Using UWB Techniques", 1992 IEEE Microwave Theory Tech. Symp., Albuquerque, NM.
3. E. G. Farr and C. E. Baum, Prepulse Associated with the TEM Feed of an Impulse Radiating Antenna, Sensor and Simulation Note 337, Appendix A, March 1992.
4. J. J. Bowman, T. B. A. Senior, and P. L. E. Uslenghi, *Electromagnetic Scattering by Simple Shapes*, Hemisphere, 1987.
5. C. E. Schensted, "Electromagnetic and Acoustic Scattering by a Semi-Infinite Body of Revolution," *Journal of Applied Physics*, Vol. 26, March 1955, pp. 306-308.
6. R. W. Latham, M. I. Sancer, and A. D. Varvatsis, Matching a Particular Pulser to a Parallel-Plate Simulator, Circuit and Electromagnetic System Design Note 18, November 1974.
7. F. C. Yang and K. S. H. Lee, Impedance of a Two Conical-Plate Transmission Line, Sensor and Simulation Note 221, November 1976.
8. W. S. Smythe, *Static and Dynamic Electricity*, Third Ed., Hemisphere, 1989, Sections 6.14 and 12.06.
9. D. V. Giri and C. E. Baum, Optimal Positioning of a Set of Peaker Arms in a Ground Plane, Circuit and Electromagnetic System Design Note 35, February 12, 1988.
10. C. Zuffada and N. Engheta, Common and Differential TEM Modes for Two Wires Above a Ground Plane, Sensor and Simulation Note 305, July 1987.
11. J. Jarem, "Electromagnetic Field Analysis of a Four-Wire Anechoic Chamber," *IEEE Trans. Antennas Propagat.*, Vol. 38, November 1990, pp. 1835-1842.
12. J. Jarem, "Analysis of a Four Parallel Wire Antenna System by the Spatial Fourier Transform," *IEEE Trans. Electromag. Compat.*, Vol. 33, August 1991, pp. 215-223.
13. C. Cheon and V. V. Liepa, Analysis and Design of Broadband Antenna for Anechoic Chamber Illumination, to appear as a Sensor and Simulation Note.
14. C. E. Baum, Impedances and Field Distributions for Symmetrical Two Wire and Four Wire Transmission Line Simulators, Sensor and Simulation Note 27, October 10, 1966.